Electronic Supplementary Material (ESI) for Journal of Materials Chemistry A.
This journal is © The Royal Society of Chemistry 2022

Electronic Supplementary Information

Binary Alloy of Functionalized Small-Molecule Acceptors of A–DA′D–A Structure for Ternary-Blend Photovoltaics Displaying High Open-Circuit Voltages and Efficiencies

*Yu-Che Lin,[a,‡] Chung-Hao Chen,[a,‡] Heng Lin,[a] Meng-Hua Li,[a] Bin Chang,[a] Ting-Fang Hsueh,[a] Bing-Shiun Tsai,[a] Yang Yang,[b] and Kung-Hwa Wei[a,c,]**

a. Department of Materials Science and Engineering, National Yang Ming Chiao Tung University, Hsinchu 30010, Taiwan.

b. Department of Material Science and Engineering, University of California, Los Angeles, CA 90095 USA

c. Center for Emergent Functional Matter Science, National Yang Ming Chiao Tung University, Hsinchu 30010, Taiwan

Yu-Che Lin and Chung-Hao Chen should be considered joint first authors

Synthetic procedure

We used the same method to prepare the precursors and **BTPO-F**.[1]
BTPO-NF The compound 1 (120 mg, 0.10 mmol) and 2-(6,7-difluoro-3-oxo-2,3-dihydro-1H-cyclopenta[b]naphthalen-1-ylidene)malononitrile (140 mg, 0.50 mmol) in dry $CHCl_3$ (20 mL) was added 0.5 ml pyridine under argon. The mixture was refluxed for 6 hrs. The solution was cooled and then quenched by pouring it into methanol. The solid in the solution was filtered and washed with methanol. The residue was purified with silica gel chromatography using hexanes to DCM/hexanes (1:1) as eluent to obtain the product compound BTPO-NF (163 mg, 95%) ^{1}H NMR (500 MHz, $CDCl_3$) δ (ppm): 9.32 (s, 2H), 9.02 (s, 2H), 8.23 (s, 2H), 7.76-7.70 (m, 4H), 4.802-4.80 (m, 4H), 4.69-4.68 (m, 4H), 2.17-2.09 (m, 4H), 1.69-1.55 (m, 16H), 1.42- 1.32 (m, 32H), 1.07-0.89 (m, 28H), 0.73-0.70 (m, 12H). ^{13}C NMR (100 MHz, $CDCl_3$, δ): 186.46, 162.74, 158.65, 154.91, 153.19, 147.39, 137.53, 137.24, 136.72, 134.52, 134.31, 132.03, 128.17, 119.77, 117.73, 115.10, 114.78, 114.59, 113.02, 112.15, 112.03, 67.58, 55.71, 39.35, 38.55, 31.89, 31.57, 30.78, 30.54, 30.47, 29.72, 29.68, 29.44, 29.40, 29.38, 28.83, 26.61, 23.06, 22.85, 22.80, 22.71, 22.51, 14.14, 14.02, 13.80.

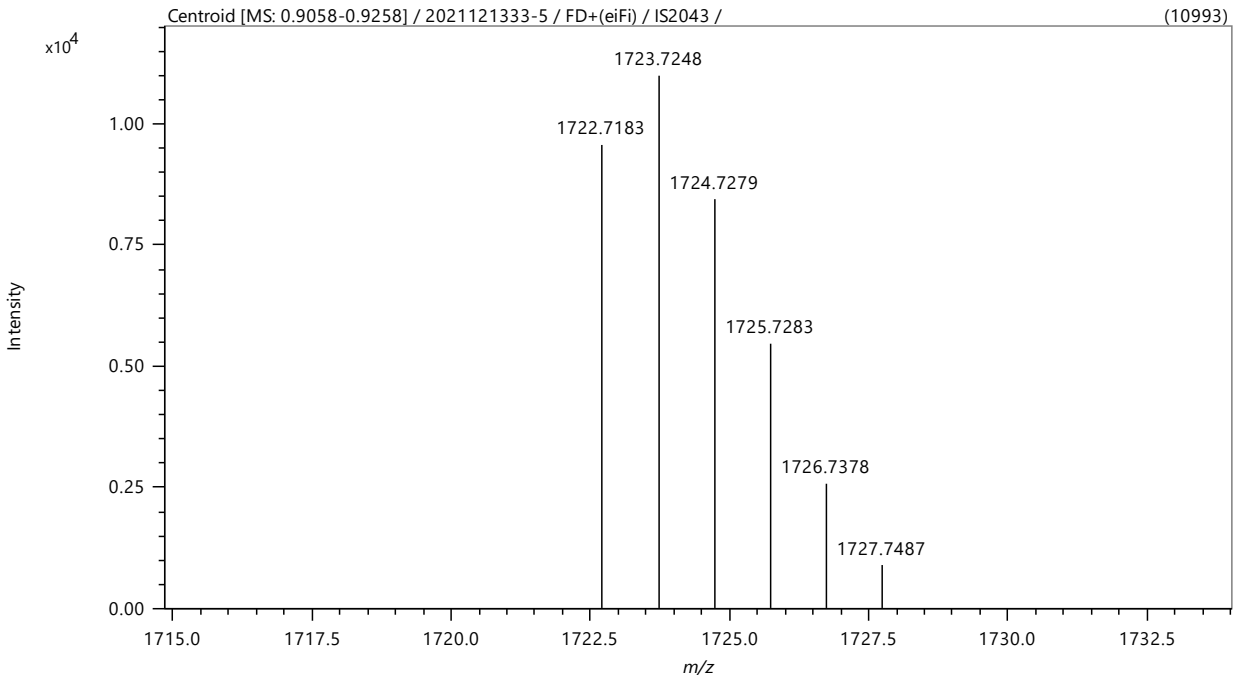

Fig. S1 Mass spectrometry data of BTPO-NF.

Measurements and Characterization

Thermogravimetric analysis (TGA) was performed with a TA Instruments Q500 apparatus; the thermal stabilities of the samples were controlled under N_2 atmosphere by measuring their weight losses while heating at a rate of 10 °C min^{-1}. The UV–Vis spectra of solid films, spin-coated from polymer solutions onto a quartz substrate, were recorded using a Hitachi U-4100 spectrophotometer. Differential scanning calorimetry (DSC) was recorded on a Mettler-Toledo, 2-HT differential scanning calorimeter. PL spectra were recorded using a HITACHI F-4500. Samples were prepared by spin-casting CF solutions onto silicon substrates; the thickness was maintained at approximately 100 nm. Cyclic voltammetry (CV) analyses of the acceptor films were performed using a BAS 100 electrochemical analyzer operated at a scan rate of 50 mV s^{-1}; the solvent was anhydrous MeCN, containing 0.1 M tetrabutylammonium hexafluorophosphate ($TBAPF_6$) as the supporting electrolyte. The potentials were measured against a Ag/Ag^+ (0.01 M $AgNO_3$) reference electrode, using the ferrocene/ferrocenium ion (Fc/Fc^+) pair as the internal standard (0.09 V). The onset potentials were determined from the crossing of two tangents drawn at the increasing and background currents of the cyclic voltammograms. HOMO energy levels were estimated relative to the energy level of the ferrocene reference (4.8 eV below vacuum level). Water contact angle measurements were performed using a water contact angle measurement system, and the surface energy was calculated using the equation of state. Topographic and phase images of the small molecule acceptors:PM6 films (surface area: 5 × 5 μm^2) were recorded using a Digital Nanoscope III atomic force microscope operated in tapping mode under ambient conditions. The thickness of the active layer of the device was measured using a VeecoDektak 150 surface profiler. GIWAXS was performed at the 23A beamline (10 keV) of the National Synchrotron Radiation Research Center (NSRRC), Hsinchu, Taiwan, using an incident angle of 0.2°. Samples were prepared by spin-casting CF solutions of the synthesized small molecule acceptors: PM6 blends onto silicon substrates. GIWAXS experiments were conducted after the solvent had evaporated entirely.

Fabrication and Characterization of Photovoltaic Devices

Zinc acetate dihydrate [$Zn(CH_3COO)_2 \cdot 2H_2O$] (1.0 g) and ethanolamine (0.28 g) were dissolved in 2-methoxyethanol (10 mL) under dynamic stirring for 12 h. Mixture solutions of the active layers were set by dissolving the small molecules (6 mg mL^{-1}) and PM6 (5mg mL^{-1}) in CF, resulting in a total concentration of 1.8 wt%. The optimal treatments involved are: 0.5% (v/v) CN followed by TA at 90 ℃ for 10 min; dual additives of 0.5% CN and 25%DTT (weight ratio relative to small molecule acceptors) followed by TA at 90℃ chloroform as processing solvent. The mixture solutions were stirred uninterruptedly in a glove box for 12 h at 90 °C to ensure complete dissolution of the synthesized small molecule acceptors and PM6. Indium tin oxide (ITO)–coated glass substrates (5 Ω cm^{-2}, Merck) were rinsed through sequential ultrasonication with detergent, acetone, DI water, and isopropanol (20 min each) and then dried under a flow of N_2. ZnO was spin-coated onto the UV ozone-treated ITO for 15 min and then annealed at 200 °C for 1 h. The substrates were transferred to a dry N_2–filled glove box. The ZnO layers were placed at a thickness of nearly 40 nm, followed by accumulation of the active layers. The active layers, formed from synthesized small molecule acceptors and PM6 blend solutions in CF, were prepared in a glove box and then spin-cast on top of the ZnO films. The active layers of synthesized small molecule acceptors and PM6 blends had thicknesses of approximately 100 nm. The BHJ devices were fabricated with structures incorporating ITO/ZnO. Device fabrication was complete after thermal evaporation of the P-type material (MoO_3, 10 nm) and the anode (Ag, 100 nm) under high vacuum (ca. 10^{-7} torr). A shadow mask was used during the thermal evaporation procedure to define a device area of 0.1 cm^2.

The current density–voltage (*J–V*) characteristics were measured using a Keithley 2400 source meter. The photocurrent was measured under simulated AM 1.5 G illumination at 100 mW cm^{-2} using a Xe lamp–based Newport 150-W solar simulator. EQEs were measured using an SRF50 system (Optosolar, Germany). For measurements of hole and electron mobilities, devices were fabricated having the structure ITO/PEDOT:PSS/active layer/Au and ITO/ZnO/binary blend/Ca/Al, respectively. The *J–V* characteristics of these diodes were recorded in the dark in a glove box under a N_2 atmosphere. Mobilities were extracted by fitting the *J–V* curves using the Mott–Gurney relationship (space charge-limited current).

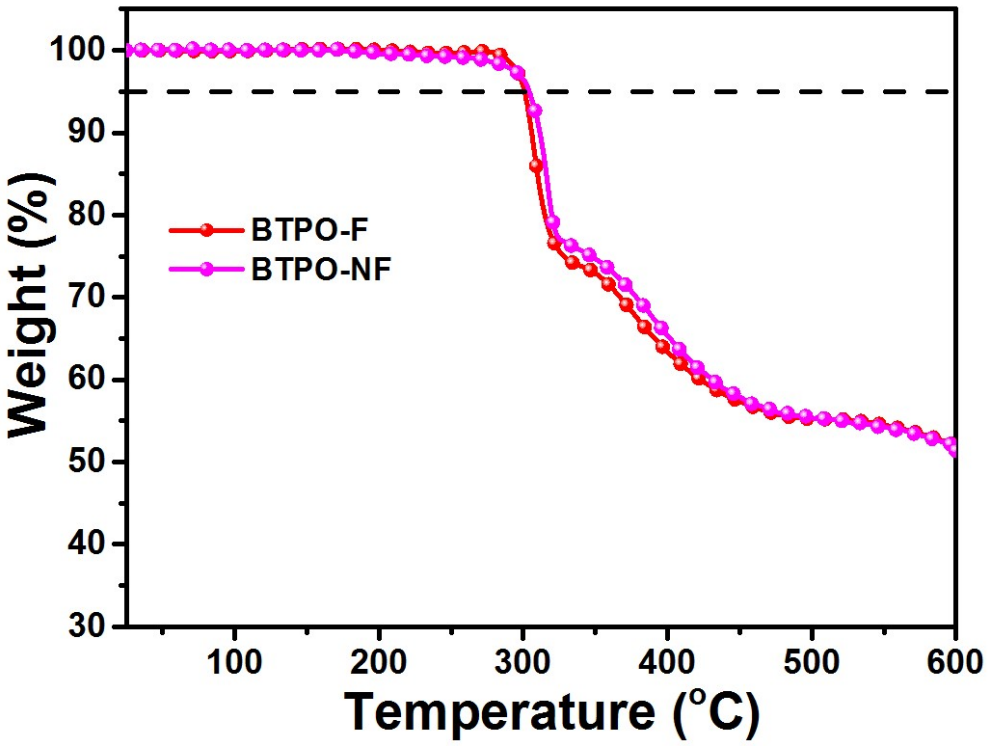

Fig. S2 TGA thermograms of two small molecules, recorded at a heating rate of 10 °C min^{-1} under a N_2 atmosphere.

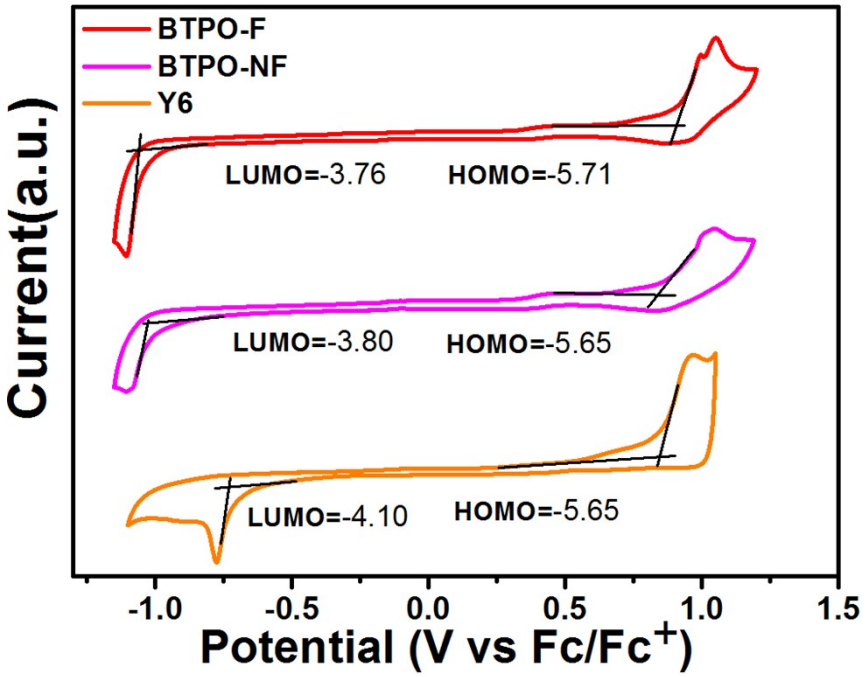

Fig. S3 Cyclic voltammograms of the synthesized small molecules and Y6 as solid films.

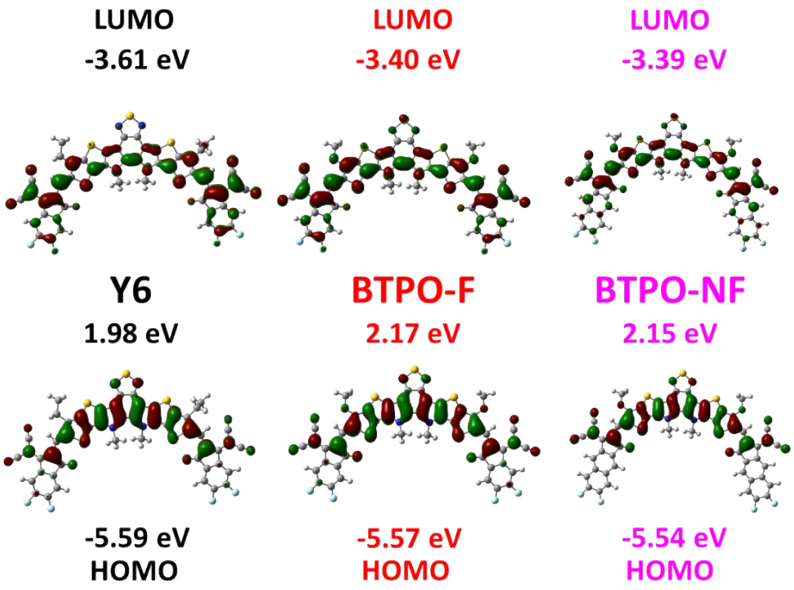

Fig. S4 HOMO and LUMO distributions with the minimum-energy conformations of Y6, BTPO-F, and BTPO-NF as calculated by Gaussian 09 at B3LYP/6-31G level.

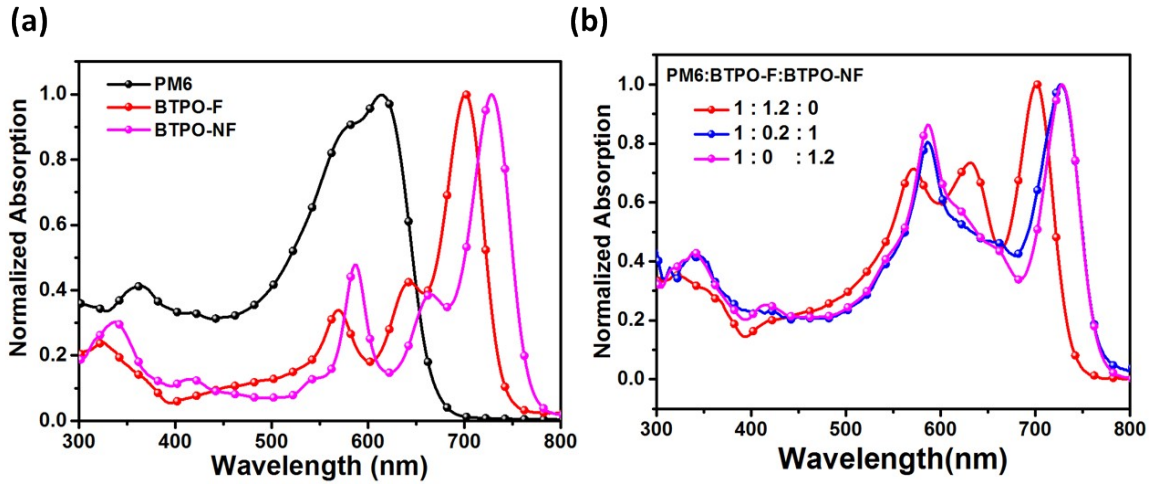

Fig. S5 (a) UV−vis absorption spectra the pure materials and (b) two kinds of binary blends, recorded from dilute solutions(1×10^{-5} M) in CF

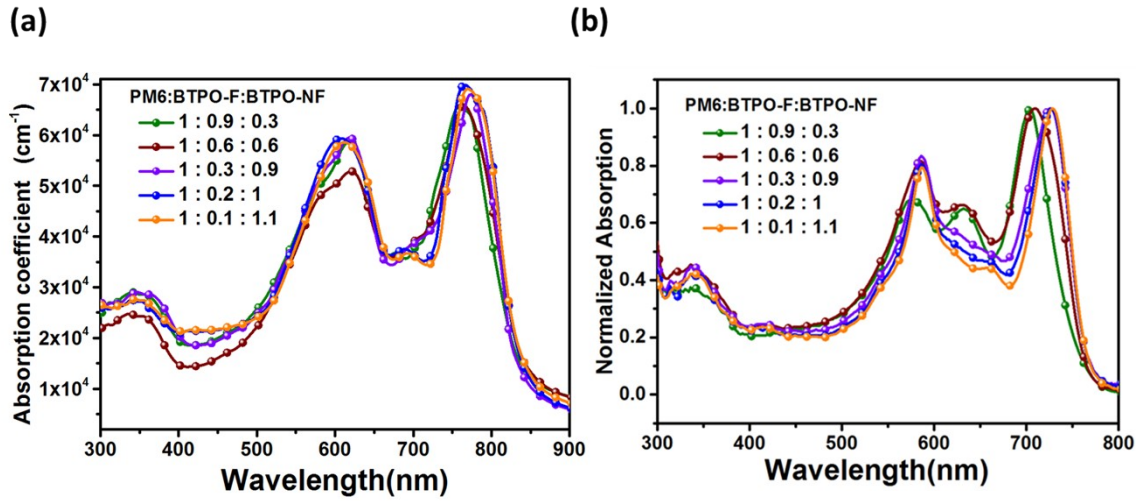

Fig. S6 UV−vis absorption spectra of ternary blends of PM6 with BTPO-NF or BTPO-F (a) solid films and (b) solution.

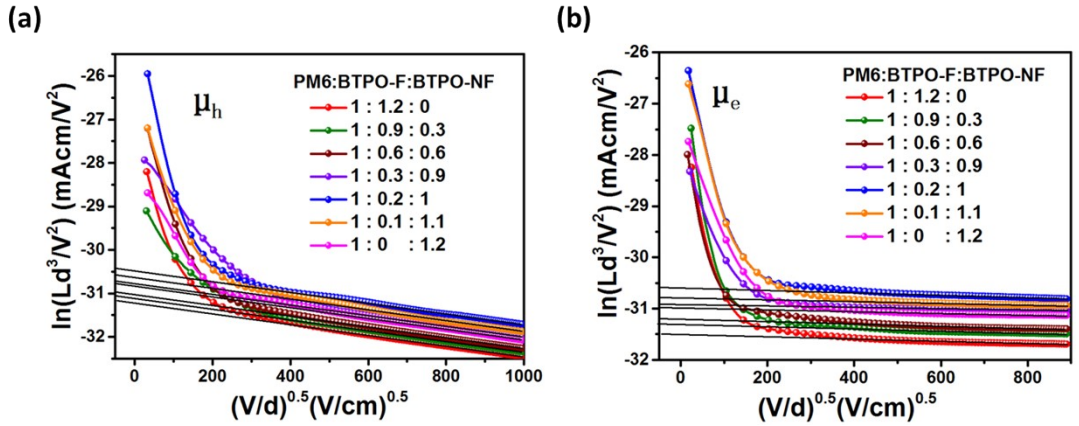

Fig. S7 (a) Hole-only and (b) electron-only devices based on the binary and ternary blend devices.

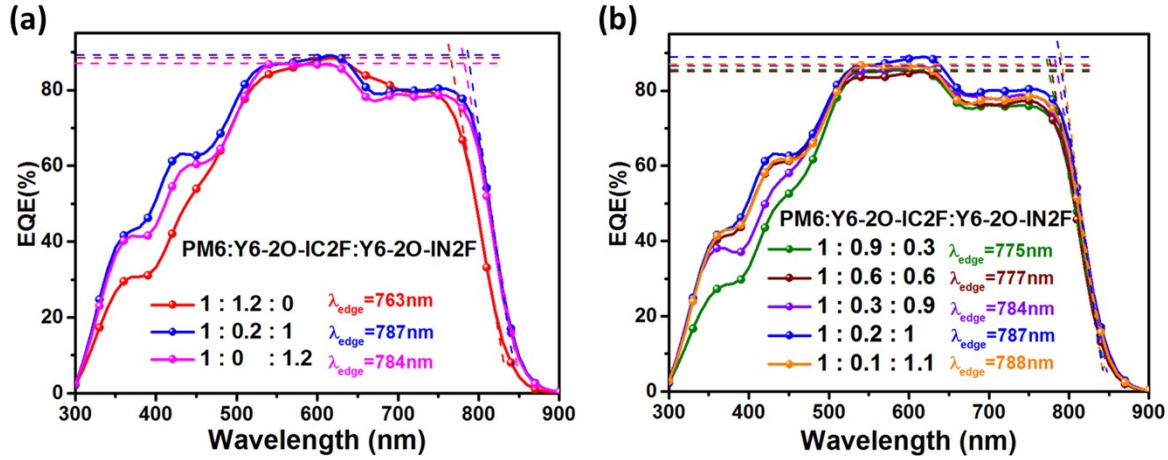

Fig. S8 The EQE curves of OPV devices incorporating (a)the two kinds of binary blends, optimized ternary blends, and (b) the five ternary blends for the graphical determination of λ_{edge}.

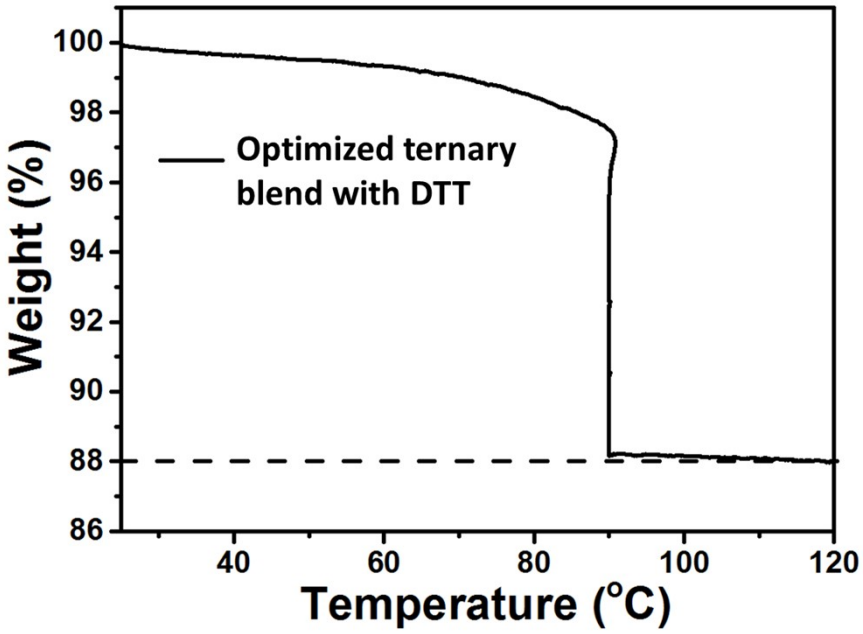

Fig. S9 TGA thermograms of the same composition to the optimized ternary blend layer, recorded at a heating rate of 10 °C min^{-1} under a N_2 atmosphere.

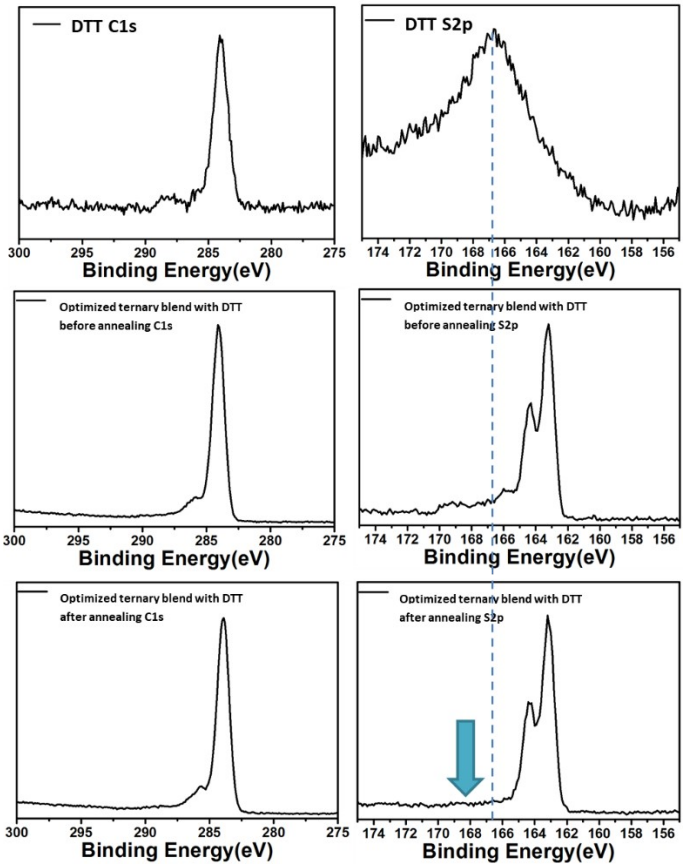

Fig. S10 High-resolution C 1s XPS spectra, and S 2p XPS spectra of the optimized ternary blend layer with/without annealing.

Table S1 The morphological parameters including crystal coherence length (CCL) of films in out-of-plane direction obtained from 2D GIWAXS patterns.

Out of plane (100)			
sample	Postion $Å^{-1}$	d-spacing Å	CCL Å
PM6	0.33	19.03	58.2
BTPO-F	0.29	21.65	102.0
BTPO-NF	0.46	13.65	79.3

Table S2 The morphological parameters of films in out-of-plane direction obtained from 2D GIWAXS patterns.

Out of plane (100)			
PM6 : BTPO-F :BTPO-NF	Postion $Å^{-1}$	d-spacing Å	CCL Å
1:1.2:0	0.31/0.39	20.25/16.10	100.3/106.8
1:0.9:0.3	0.31/0.37	20.25/16.97	99.9/110.2
1:0.6:0.6	0.31/0.37	20.25/16.97	99.9/118.4
1:0.3:0.9	0.31/0.33	20.25/19.03	90.9/129.0
1:0.2:1	0.31/0.33	20.25/19.03	70.8/166.4
1:0.1:1.1	0.31/0.33	20.25/19.03	71.2/110.4
1:0:1.2	0.33	19.03	90.7

Table S3 The energy levels and bandgaps, collected from various measurement.

Bandgap (Eg) orλ	**Y6 (eV)**	**BTPO-F (eV)**	**BTPO-NF (eV)**
$\lambda_{max\ abs}$(solution)	725 nm	703 nm	729 nm
$\lambda_{max\ abs}$(film)	825 nm	760 nm	790 nm
$\Delta\lambda_{max\ abs}$ (solution to film)	100 nm	57 nm	61 nm
UV-Vis optical (Eg) solid film,	1.33	1.50	1.45
DFT (Eg) single molecule, eV	1.98	2.17	2.15
CV (Eg) solid film, eV	1.55	1.95	1.85
$\Delta Eg = (Eg_{DFT}-Eg_{CV})$, eV	0.43 eV	0.22	0.30

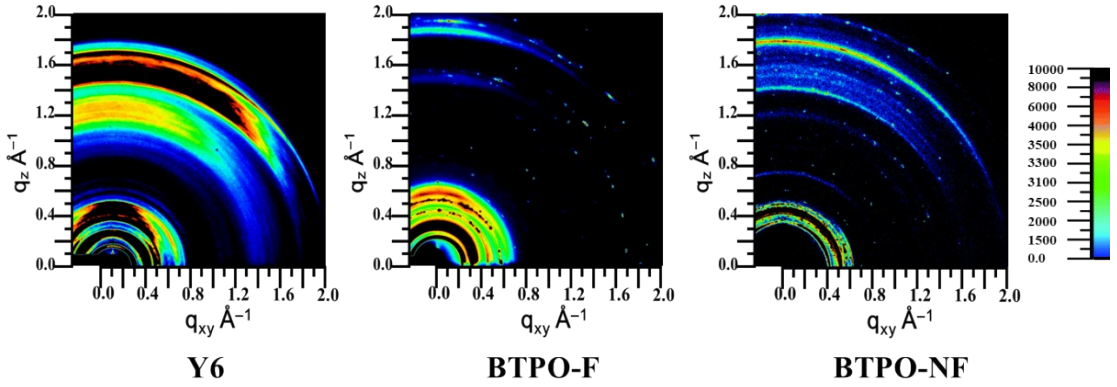

Fig. S11 2-D GIWAXS patterns of Y6, BTPO-F, and BTPO-NF.

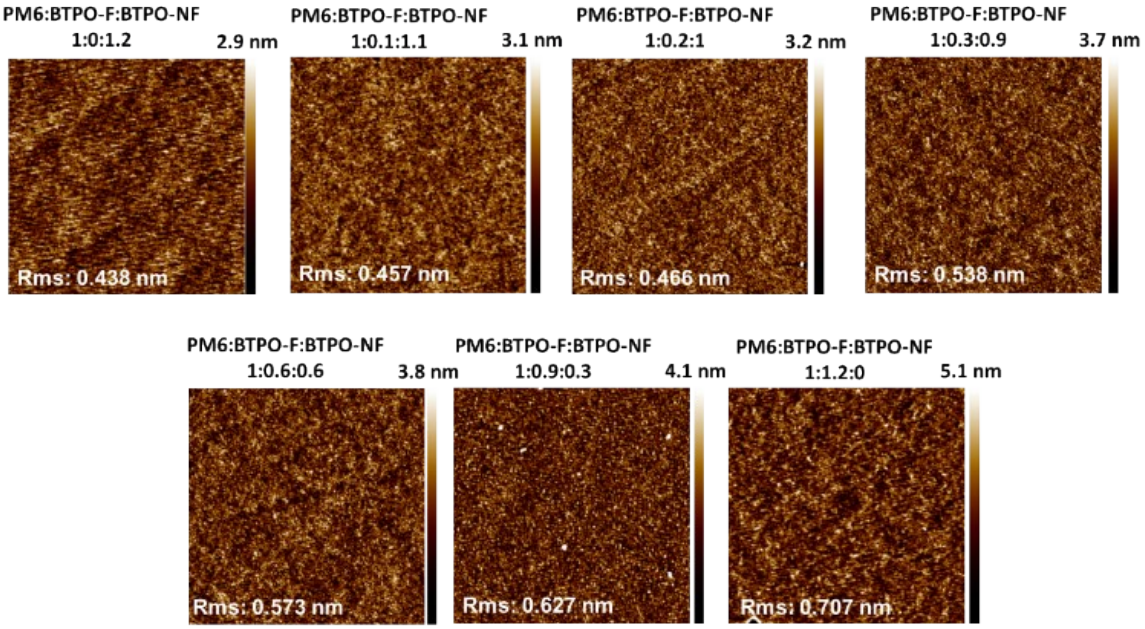

Fig. S12 AFM height images (5 × 5 μm) of the blend films.

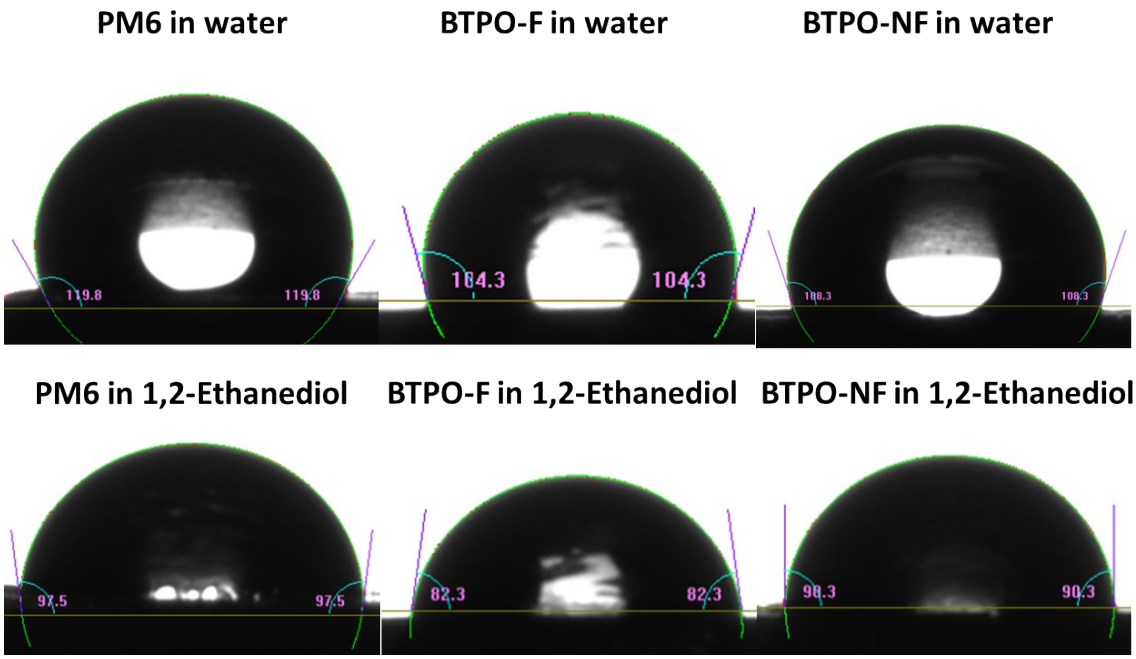

Fig. S13 The contact angle of the two synthesized small molecular and PM6.

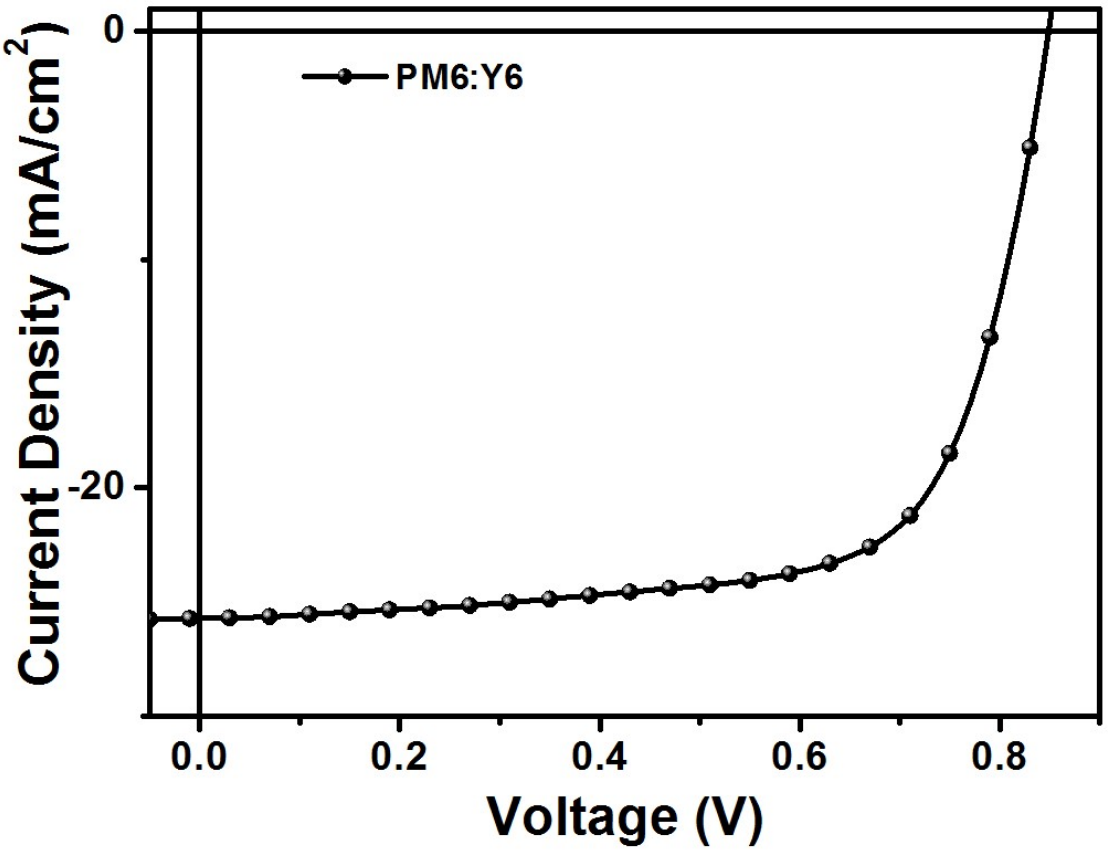

Fig. S14 *J–V* characteristics of PM6:Y6 devices

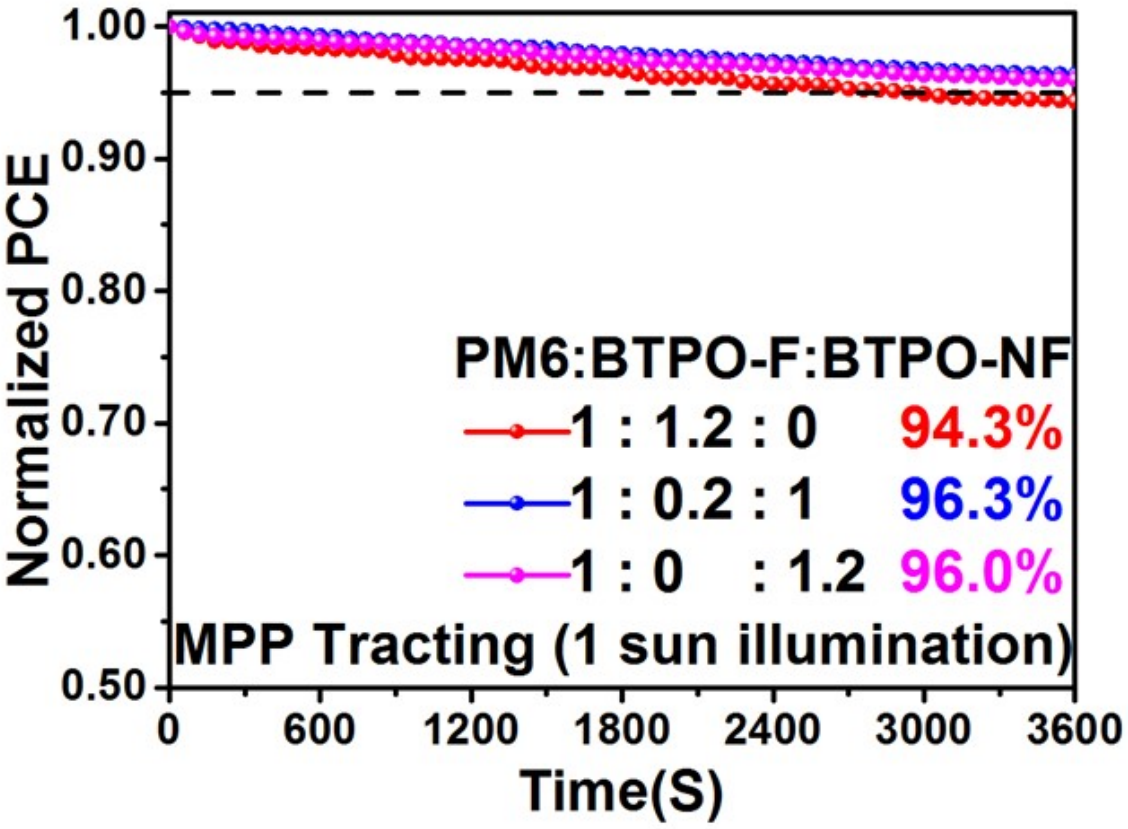

Fig. S15 The normalized power conversion efficiencies of binary and ternary blends of PM6 with BTPO-F and/or BTPO-NF at various weight ratios varying with time under 1 sun illumination in a nitrogen environment.

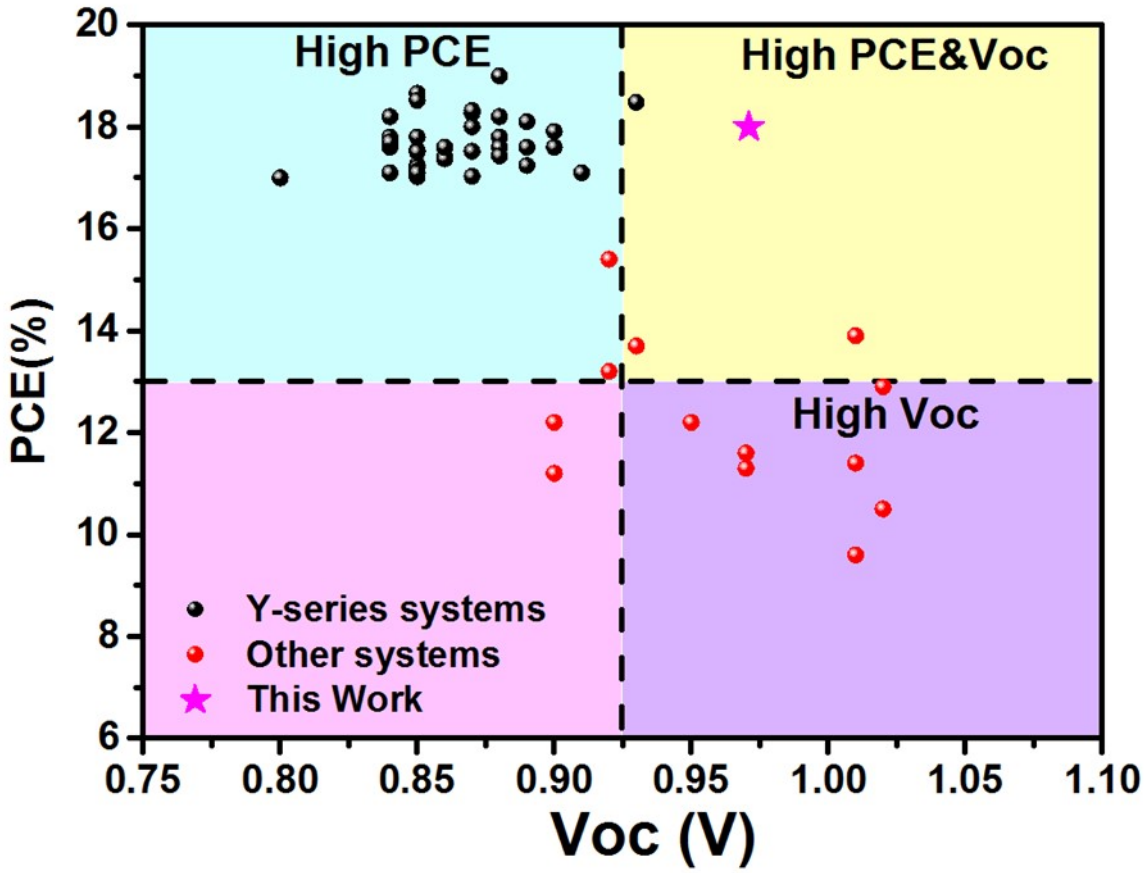

Fig. S16 Plots of the PCE against V_{OC} for various systems.

Table S4 Detailed photovoltaic parameters of binary blend OPVs with different D:A ratio.

Active layer	D:A ratio	V_{OC} (V)	J_{SC} (mA cm^{-2})	FF (%)	PCE_{max} (PCE_{avg} [a], %)
PM6 :BTPO-F	1:1	0.951(0.948±0.002)	19.86(19.60±0.11)	70.9(70.5±0.1)	13.39(13.09±0.15)
	1:1.1	0.956(0.954±0.001)	20.01(19.68±0.13)	72.6(71.9±0.2)	13.88(13.49±0.19)
	1:1.2	0.961(0.958±0.002)	20.24(20.01±0.08)	73.1(72.8±0.1)	14.21(13.96±0.12)
	1:1.3	0.973(0.970±0.002)	18.97(18.55±0.07)	71.3(70.9±0.1)	13.16(12.75±0.28)
	1:1.4	0.986(0.983±0.002)	17.69(17.47±0.17)	65.2(64.7±0.1)	11.37(11.11±0.21)
PM6 :BTPO-NF	1:1	0.941(0.939±0.001)	20.88(20.43±0.15)	72.1(71.5±0.2)	14.16(13.71±0.11)
	1:1.1	0.945(0.943±0.001)	20.95(20.68±0.09)	73.4(72.8±0.1)	14.53(14.19±0.21)
	1:1.2	0.952(0.950±0.001)	21.01(20.79±0.14)	75.9(74.6±0.2)	15.18(14.73±0.27)
	1:1.3	0.967(0.965±0.001)	20.47(20.02±0.12)	72.5(71.3±0.1)	14.35(13.77±0.33)
	1:1.4	0.971(0.969±0.001)	18.12(17.47±0.31)	69.3(68.6±0.1)	12.19(11.61±0.29)

[a])Ten devices were fabricated in each case.

Table S5 Detailed photovoltaic parameters of binary blend OPVs under the same optimal donor/receptor weight ratio of 1:1.2 with different concentration using CF as solvent

Active layer	Concentration (mg/mL)	V_{OC} (V)	J_{SC} (mAcm^{-2})	FF (%)	PCE_{max} (PCE_{avg} [a], %)
PM6 :BTPO-F	1.8	0.959(0.956±0.002)	19.86(19.68±0.08)	70.9(70.6±0.1)	13.50(13.28±0.09)
	2.0	0.961(0.958±0.001)	20.01(19.89±0.07)	72.6(71.9±0.1)	13.96(13.71±0.06)
	2.2	0.961(0.958±0.002)	20.24(20.01±0.08)	73.1(72.8±0.1)	14.21(13.96±0.12)
	2.4	0.960(0.958±0.001)	19.97(19.91±0.04)	71.3(71.1±0.1)	13.67(13.55±0.11)
	2.6	0.959(0.956±0.002)	19.81(19.63±0.09)	70.9(70.5±0.2)	13.47(13.23±0.15)
PM6 :BTPO-NF	1.8	0.951(0.949±0.001)	20.97(20.74±0.18)	73.1(72.8±0.2)	14.58(14.35±0.06)
	2.0	0.952(0.950±0.001)	20.98(20.81±0.11)	74.6(74.3±0.1)	14.89(14.68±0.17)
	1:1.2	0.952(0.949±0.002)	21.01(20.93±0.05)	75.9(74.6±0.3)	15.18(14.73±0.27)
	2.4	0.950(0.948±0.001)	20.87(20.65±0.12)	73.6(73.1±0.3)	14.59(14.31±0.16)
	2.6	0.949(0.947±0.001)	20.81(20.51±0.21)	71.6(71.1±0.4)	14.14(13.81±0.08)

[a] Ten devices were fabricated in each case.

Table S6 Detailed photovoltaic parameters of binary and ternary blend OPVs under different additive treatments.

Active layer	*Additive*	V_{OC} (V)	J_{SC} (mA cm^{-2})	FF (%)	PCE_{max} (PCE_{avg} [a], %)
PM6:BTPO-F	0.5%CN	0.965(0.963±0.001)	21.08(20.91±0.07)	76.5(76.3±0.1)	15.57(15.36±0.10)
	25%DTT	0.971(0.969±0.002)	21.29(21.11±0.05)	76.9(76.7±0.1)	15.89(15.68±0.14)
	0.5%CN +25%DTT	0.989(0.986+0.002)	21.32(21.26±0.05)	77.1(76.9±0.1)	16.23(16.12±0.05)
PM6:BTPO-NF	0.5%CN	0.957(0.955±0.001)	21.68(21.45±0.09)	78.2(78.1±0.1)	16.22(15.99±0.18)
	25%DTT	0.960(0.958±0.001)	22.09(21.93±0.08)	78.8(78.6±0.1)	16.71(16.51±0.13)
	0.5%CN +25%DTT	0.961(0.959±0.002)	22.43(22.29±0.10)	79.4(79.1±0.2)	17.11(16.90±0.15)
PM6:BTPO-F:BTPO-NF=1:0.2:1	0.5%CN	0.963(0.961±0.001)	22.39(22.29±0.07)	77.9(77.7±0.1)	16.80(16.64±0.13)
	25%DTT	0.968(0.966±0.001)	22.86(22.73±0.05)	78.4(78.2±0.1)	17.34(17.17±0.10)
	0.5%CN +25%DTT	0.971(0.969±0.001)	23.21(23.29±0.04)	79.6(79.4±0.1)	18.00(17.80±0.09)

[a] Twenty devices were fabricated in each case.

Table S7 Detailed photovoltaic parameters of binary and ternary blend OPVs treated with dual additives of CN and DTT under different rotate speed for casting active-layers.

Active layer	RPM	V_{OC} (V)	J_{SC} (mA cm^{-2})	FF (%)	PCE_{max} (PCE_{avg} [a], %)
PM6 :BTPO-F	2500	0.988(0.985±0.001)	20.89(20.81±0.04)	74.9(74.7±0.1)	15.45(15.31±0.05)
	3000	0.987(0.984±0.001)	21.11(21.05±0.03)	76.5(76.3±0.1)	15.93(15.81±0.04)
	3500	0.989(0.986+0.002)	21.32(21.26±0.05)	77.1(76.9±0.1)	16.23(16.12±0.05)
	4000	0.988(0.986±0.001)	21.08(21.04±0.04)	76.8(76.6±0.1)	15.99(15.89±0.03)
	4500	0.989(0.986±0.001)	20.77(20.69±0.06)	75.2(74.9±0.1)	15.44(15.27±0.06)
PM6 :BTPO-NF	2500	0.959(0.956±0.002)	20.95(20.87±0.06)	76.4(76.1±0.2)	15.34(15.18±0.05)
	3000	0.961(0.959±0.001)	22.11(21.95±0.07)	78.5(78.3±0.1)	16.68(16.48±0.11)
	3500	0.961(0.959±0.002)	22.43(22.29±0.10)	79.4(79.1±0.2)	17.11(16.90±0.15)
	4000	0.959(0.957±0.001)	22.03(21.91±0.08)	79.1(78.8±0.2)	16.71(16.52±0.12)
	4500	0.960(0.958±0.001)	21.05(20.84±0.11)	77.2(77.0±0.1)	15.6(15.37±0.14)
PM6 :BTPO-F :BTPO-NF=1:0.2:1	2500	0.970(0.969±0.001)	21.58(21.41±0.06)	77.2(77.0±0.1)	16.15(15.98±0.13)
	3000	0.971(0.968±0.001)	22.01(21.83±0.09)	78.8(78.6±0.1)	16.84(16.66±0.19)
	3500	0.971(0.969±0.001)	23.21(23.29±0.04)	79.6(79.4±0.1)	18.00(17.80±0.09)
	4000	0.970(0.969±0.001)	21.97(21.84±0.11)	78.6(78.3±0.2)	16.75(16.56±0.12)
	4500	0.970(0.969±0.001)	21.67(21.51±0.08)	77.1(76.8±0.2)	16.20(16.01±0.14)

[a])Ten devices were fabricated in each case.

Table S8 The state-of-the-art ternay blend photovoltaics incorporating Y-series as small molecule acceptors.

	Voc	Jsc	FF	PCE	Ref.
PM6:D18:L8-BO	0.90	26.7	81.9	19.6	2
PM6:L8-BO:BTP-H2	0.89	26.7	80.7	19.2	3
PBQx-TF:eC9-2Cl:F-BTA3	0.88	26.7	81.0	19.0	4
PM6:BTP-eC9:L8-BO-F	0.85	27.3	80.0	18.6	5
PB2F:PM6:BTP-eC9	0.86	26.8	80.4	18.6	6
PM6:BTP-eC9:BTP-S2	0.87	26.7	79.4	18.6	7
PM6:Y6-1O:BO-4Cl	0.85	27.4	79.0	18.5	8
PM6:BTP-eC9:BTP-F	0.86	27.0	79.9	18.4	9
PM6:PM6-Si30:C9	0.87	26.9	77.9	18.2	10
PM6 : L8-BO.	0.89	25.8	78.6	18.1	11
PM6:BTPO-F:BTPO-NF	**0.97**	**23.3**	**79.6**	**18.0**	**This Work**
PM6:Y6:AQx-3	0.87	26.8	77.2	18.0	12
PM6:BTP-eC9:$PC_{71}BM$	0.845	26.94	79.2	18.0	13
D18-Cl : Y6-1O:Y6	0.90	25.8	76.9	17.9	14
PM6:Y6:Y6-BO:PCBM	0.85	26.6	78.5	17.8	15
PM6:CH1007:BT-4BO	0.88	26.9	75.3	17.8	16
PTQ10:BTP-Ph:BTP-Th	0.88	25.2	78.6	17.6	17
PM6: Y6-1O: PC71BM	0.90	24.9	78.5	17.6	18
PM6:N3:PC71BM	0.84	26.7	78.0	17.6	19
PM6:Y6:BTIC-EH-2ThBr	0.85	26.4	77.9	17.5	20
PM6:S3:Y6	0.85	25.8	79.1	17.5	21
PM6:Y6:C8-DTC	0.87	26.5	75.6	17.5	22
PM6: Y6-O2BO: Y6	0.87	25.2	78.9	17.5	1
PM6:Y6:BTP-S2	0.88	26.2	75.8	17.4	23
PM6:Y6:ITCPTC	0.86	25.6	78.8	17.4	24
PM6 : TiC12 : Y6	0.85	26.8	75.4	17.2	25
PM6:M36:MQ5	0.89	25.3	76.2	17.2	26
PhI-Se:PM6:Y6:$PC_{71}BM$	0.85	26.3	76.8	17.2	27
PM6:DRTB-T-C4:Y6	0.85	24.8	81.3	17.1	28
PM6:ABP6T-4F:CH1007	0.85	26.6	75.8	17.1	29
PM6 : Y6:BTP-M	0.87	26.5	73.4	17.0	30
PM6 :Y6:$PC_{71}BM$/CIL:BCP	0.85	25.9	77.2	17.0	31

Table S9 The state-of-the-art binary blend photovoltaics incorporating Y-series as small molecule acceptors.

	Voc	Jsc	FF	PCE	Ref.
PM6:BTP-H2	0.93	25.3	78.5	18.5	3
PM6:BTP-eC9	0.85	27.1	80.8	18.5	32
PM6:AC9	0.87	26.7	79.0	18.4	33
PM6:L8-BO	0.87	25.7	81.5	18.3	34
PM6: TP-4F-P2EH	0.88	25.8	80.0	18.2	35
PM6:BTP-4F-C5-16	0.84	27.8	77.6	18.2	36
PM6:BTP-eC9	0.84	26.2	81.1	17.8	37
PM6:BTP-4Cl	0.84	26.7	79.0	17.7	38
PM6-Tz20:Y6	0.86	27.3	75.0	17.6	39
PM6:BTP-T-3Cl	0.89	26.0	75.8	17.6	40
PM6: A-WSSe-Cl	0.85	26.5	77.5	17.5	41
PM6:BTP1O-4Cl-C12	0.91	23.8	78.8	17.1	42
PM6:BTA-C5	0.85	26.5	76.2	17.1	43
SZ4:N3	0.84	26.0	77.4	17.1	44
PM6:mBzS-4F	0.80	27.7	76.3	17.0	45

Table S10 Device parameters for OSCs with high V_{OC}.

	Voc	Jsc	FF	PCE	Ref.
PE31:BTA5	1.11	13.6	66	10.0	46
PBDB-T: DT-BOC6	1.01	17.5	54	9.6	47
PBDB-T: ITOIC-2F	0.9	21.0	65	12.2	48
J52-Cl:F-BTA3	1.15	12.8	68	10.1	49
PM6: IDTN	0.95	16.5	78	12.2	50
PBDB-T: ITIC	0.90	16.8	74	11.2	51
PBDB-T: ITC6-IC	0.97	16.4	73	11.6	52
PBDB-T: IT-DM	0.97	16.4	71	11.3	53
PBDB-T: ITCC	1.01	15.9	71	11.4	54
PM6: IT-M	1.02	15.7	65	10.5	55
PBTA-PSF:ITIC	1.01	18.5	74	13.9	56
PM6: DTTC-4Cl	0.92	22.6	74	15.4	57
PM6: TSeTIC	0.93	19.4	76	13.7	58
PBDFP- Bz:IT- M	1.02	18.6	69	12.9	59
PM6: ITIC-2Cl	0.92	19.0	75	13.2	60

References

1. J. Liang, M. Pan, Z. Wang, J. Zhang, F. Bai, R. Ma, L. Ding, Y. Chen, X. Li, H. Ade, H. Yan, *Chem. Mater.,* 2022, **34**, 2059.
2. L. Zhu, M. Zhang, J. Xu, C. Li, J. Yan, G. Zhou, W. Zhong, T. Hao, J. Song, X. Xue, Z. Zhou, R. Zeng, H. Zhu, C.-C. Chen, R. C. I. MacKenzie, Y. Zou, J. Nelson, Y. Zhang, Y. Sun, F. Liu, *Nat. Mater.,* 2022, **21**, 656.
3. C. He, Y. Pan, Y. Ouyang, Q. Shen, Y. Gao, K. Yan, J. Fang, Y. Chen, C.-Q. Ma, J. Min, C. Zhang, L. Zuo, H. Chen, *Energy Environ. Sci.*, 2022, doi.org/10.1039/D2EE00595F.

4. Y. Cui, Y. Xu, H. Yao, P. Bi, L. Hong, J. Zhang, Y. Zu, T. Zhang, J. Qin, J. Ren, Z. Chen, C.He, X. Hao, Z. Wei, J. Hou, *Adv.Mater.*, 2021, **33**, 2102420.
5. Y. Cai, Y. Li, R. Wang, H. Wu, Z. Chen, J. Zhang, Z. Ma, X. Hao, Y.Zhao, C. Zhang, F. Huang, Y. Sun, *Adv. Mater.,* 2021, **33**, 2101733.
6. T. Zhang, C. An, P. Bi, Q. Lv, J. Qin, L. Hong, Y. Cui, S. Zhang, J. Hou, *Adv. Energy Mater.*, 2021, **11**, 2101705
7. Y. Li, Y. Guo, Z. Chen, L. Zhan, C. He, Z. Bi, N. Yao, S. Li, G. Zhou, Y. Yi, Y. (M.) Yang, H. Zhu, W. Ma, F. Gao, F. Zhang, L. Zuo, H. Chen, *Energy Environ. Sci.*, 2022, **15**, 855.
8. D. Wang, G. Zhou, Y. Li, K. Yan, L. Zhan, H. Zhu, X. Lu, H. Chen, C.-Z. Li, *Adv. Funct. Mater*., 2022, **32**, 2107827.
9. Y. Li, Yunhao Cai, Y. Xie, J. Song, H. Wu, Z. Tang, J. Zhang, F. Huang, Y. Sun, *Energy Environ. Sci*., 2021, **14**, 5009–5016.
10. W. Peng, Y. Lin, S. Y. Jeong, Z. Genene, A. Magomedov, H. Y. Woo, C. Chen, W. Wahyudi, Q. Tao, J. Deng, Y. Han, V. Getautis, W. Zhu, T. D. Anthopoulos, E. Wang, *Nano Energy*, 2022, **92**, 106681.
11. X. Xu, L. Yu, H. Meng, L. Dai, H. Yan, R. Li, Q. Peng, *Adv. Funct. Mater.,* 2022, **32**, 2108797.
12. F. Liu, L. Zhou, W. Liu, Z. Zhou, Q. Yue, W. Zheng, R. Sun, W. Liu, S. Xu, H. Fan, L. Feng, Y. Yi, W.Zhang, X. Zhu, *Adv.Mater.,* 2021, **33**, 2100830.
13. Y. Lin, M. I. Nugraha, Y. Firdaus, A. D. Scaccabarozzi, F. Aniés, A.-H. Emwas, E. Yengel, X. Zheng, J. Liu, W. Wahyudi, E. Yarali, H. Faber, O. M. Bakr, L. Tsetseris, M. Heeney, T. D. Anthopoulos, *ACS Energy Lett.*, 2020, **5**, 2935.
14. X. Ma, A. Zeng, J. Gao, Z. Hu, C. Xu, J. H. Son, S. Y. Jeong, C. Zhang, M. Li, K. Wang, H. Yan, Z. Ma, Y. Wang, H. Y. Woo, F. Zhang, *Natl Sci Rev.*, 2021, **8**, nwaa305.
15. M. Zhang, L. Zhu, T. Hao, G. Zhou, C. Qiu, Z. Zhao, N. Hartmann, B. Xiao, Y. Zou, W. Feng, H. Zhu, M. Zhang, Y. Zhang, Y. Li, T. P. Russell, F. Liu, *Adv.Mater.,* 2021, **33**, 2007177.
16. B. Fan, W. Gao, Y. Wang, W. Zhong, F. Lin, W. J. Li, F. Huang, K.-M. Yu, A. K.-Y. Jen, *ACS Energy Lett.,* 2021, **6**, 3522.
17. Y. Chang, J. Zhang, Y. Chen, G. Chai, X. Xu, L. Yu, R. Ma, H. Yu, T. Liu, P. Liu, Q. Peng, H. Yan, *Adv. Energy Mater.,* **2021**, *11*, 2100079.
18. Y. Chen, F. Bai, Z. Peng, L. Zhu, J. Zhang, X. Zou, Y. Qin, H. K. Kim, J. Yuan, L.-K. Ma, J. Zhang, H. Yu, P. C. Y. Chow, F. Huang, Y. Zou, H. Ade, F. Liu, H. Yan, *Adv. Energy Mater.,* 2021, **11**, 2003141.
19. Y. Qin, Y. Xu, Z. Peng, J. Hou, H. Ade, *Adv. Funct. Mater.,* 2020, **30**, 2005011.
20. C. Cao, H. Lai, H. Chen, Y. Zhu, M. Pu, N. Zheng, F. He, *J. Mater. Chem. A*, 2021, **9**, 16418.
21. Q. An, J. Wang, X. Ma, J. Gao , Z. Hu , B. Liu , H. Sun , X. Guo , X. Zhang, F. Zhang, *Energy Environ. Sci.,* 2020, **13**, 5039.
22. Q. Ma, Z. Jia, L. Meng, J. Zhang, H. Zhang, W. Huang, J. Yuan, F. Gao, Y. Wan, Z. Zhang, Y. Li, *Nano energy*, 2020, **78**,105272.
23. S. Li, L. Zhan, Y. Jin, G. Zhou, T.-K. Lau, R. Qin, M. Shi, C.-Z. Li, H. Zhu, X. Lu, F. Zhang, H. Chen, *Adv.Mater.,* 2020, **32**, 2001160.
24. R. Ma, T. Liu, Z. Luo, K. Gao, K. Chen, G. Zhang, W. Gao, Y. Xiao, T.-K. Lau, Q. Fan, Y. Chen, L.-K. Ma, H. Sun, G. Cai, T. Yang, X. Lu, E. Wang, C. Yang, A. K.-Y. Jen, H.Yan, *ACS Energy Lett.,* 2020, **5**, 2711.
25. W. Tang, W. Peng, M. Zhu, H. Jiang, W. Wang, H. Xia, R. Yang, O. Inganas, H. Tan, Q. Bian, E. Wang, W. Zhu, *J. Mater. Chem. A*, 2021, **9**, 20493.

26. X. Ma, C. Tang, Y. Ma, X. Zhu, J. Wang, J. Gao, C. Xu, Y. Wang, J. Zhang, Q. Zheng, F. Zhang, *ACS Appl. Mater. Interfaces,* 2021, **13**, 57684−57692.
27. W. Zhang, J. Huang, J. Xu, M. Han, D. Su, N. Wu, C. Zhang, A. Xu, C. Zhan, *Adv. Energy Mater.,* 2020, **10**, 2001436.
28. D. Li, L. Zhu, X. Liu, W. Xiao, J. Yang, R. Ma, L. Ding, F. Liu, C. Duan, M. Fahlman, Q. Bao, *Adv.Mater.,* 2020, **32**, 2002344.
29. W. Gao, B. Fan, F. Qi, F. Lin, R. Sun, X. Xia, J. Gao, C. Zhong, X. Lu, J. Min, F. Zhang, Z. Zhu, J. Luo, A. K.-Y. Jen, *Adv. Funct. Mater.,* 2021, **31**, 2104369.
30. L. Zhan, S. Li, T.-K. Lau , Y. Cui, X. Lu, M Shi, C.-Z. Li, H. Li, J. Hou, H. Chen, *Energy Environ. Sci.*, 2020, **13**, 635-645.
31. T. Liu, L. Sun, C. Xie, W. Wang, F. Qina, Y. Zhou, *J. Mater. Chem. A*, 2021, **9**, 23269-23275.
32. X. Xiong, X. Xue, M. Zhang, T. Hao, Z. Han, Y. Sun, Y. Zhang, F. Liu, S. Pei, L. Zhu, *ACS Energy Lett.*, 2021, **6**, 3582.
33. C. He, Z. Bi, Z. Chen, J. Guo, X. Xia, X. Lu, J. Min, H. Zhu, W. Ma, L. Zuo, H. Chen, *Adv. Funct. Mater.*, 2022, **32**, 2112511.
34. C. Li, J. Zhou, J. Song, J. Xu, H. Zhang, X. Zhang, J. Guo, L. Zhu, D. Wei, G. Han, J. Min , Y. Zhang, Z. Xie, Y. Yi, H Yan, F. Gao, F. Liu, Y. Sun, *Nature Energ*., 2021, **6**, 605-613.
35. J. Zhang, F. Bai, I. Angunawela ,X. Xu, S. Luo, C. Li, G.Chai, H. Yu, Y. Chen, H. Hu, Z. Ma, H. Ade, H. Yan, *Adv. Energy Mater*., 2021, **11**, 2102596.
36. L. Wang, C. Guo, X. Zhang, S. Cheng, D. Li, J. Cai, C. Chen, Y. Fu, J. Zhou, H. Qin, D. Liu, T. Wang, *Chem. Mater*., 2021, **33**, 8854.
37. Y. Cui, H. Yao, J. Zhang, K. Xian, T. Zhang, L. Hong, Y. Wang, Y. Xu, K. Ma, C. An, C. He, Z. Wei, F. Gao, J. Hou, *Adv.Mater*., 2020, **32**, 1908205.
38. L. Ma, H. Yao, J. Wang, Y. Xu, M. Gao,Y. Zu, Y. Cui, S. Zhang, L. Ye, J. Hou, *Angew. Chem. Int. Ed*., 2021, **60**, 15988.
39. X. Guo, Q. Fan, J. Wu, G. weiLi, Z. Peng, W. Su, J. Lin, L. Hou, Y. Qin, H. Ade, L. Ye, M. Zhang, Y. Li, *Angew. Chem. Int. Ed*., 2021, **60**, 2322.
40. Y. Pan, X. Zheng, J. Guo, Z. Chen, S. Li, C. He, S. Ye, X. Xia, S. Wang, X. Lu, H. Zhu, J. Min, L. Zuo, M. Shi, H. Chen, *Adv. Funct. Mater.*, 2022, **32**, 2108614.
41. C. Yang, Q. An, H. RuiBai, H. FuZhi, H. SookRyu, A. Mahmood, X. Zhao, S. Zhang,H. Y. Woo, J.-L. Wang, *Angew. Chem. Int. Ed*., 2021, **60**, 19241.
42. Y. Chen, R. Ma, T. Liu, Y. Xiao, H. K. Kim, J. Zhang, C. Ma, H. Sun, F. Bai, X. Guo, K. S. Wong, X. Lu, H. Yan, *Adv. Energy Mater*., 2021, **11**, 2003777.
43. H. Chen, X. Xia, J. Yuan, Q. Wei, W. Liu, Z. Li, C. Zhu, X. Wang, H. Guan, X. Lu, Y. Li, Y. Zou, *ACS Appl. Mater. Interfaces*, 2021, **13**, 36053.
44. J. Liang, M. Pan, G. Chai, Z. Peng, J. Zhang, S. Luo, Q. Han, Y. Chen, A. Shang, F. Bai, Y. Xu, H. Yu, J. Y. L. Lai, Q. Chen, M. Zhang, H. Ade, H. Yan, *Adv. Mater*., 2020, **32**, 2003500.
45. F. Qi, K. Jiang, F. Lin, Z. Wu, H. Zhang, W. Gao, Y. Li, Z. Cai, H. Y. Woo, Z. Zhu, A. K.-Y. Jen, *ACS Energy Lett*., 2021, **6**, 9.
46. T. Dai, P. Lei, B. Zhang, A. Tang, Y. Geng, Q. Zeng, E. Zhou, *ACS Appl. Mater. Interfaces,* 2021, **13**, 21556.
47. Y. Liu, Z. Zhang, S. Feng, M. Li, L. Wu, R. Hou, X. Xu, X. Chen, Z. Bo, *J. Am. Chem. Soc*., 2017, **139**, 3356.
48. Y. Liu, C. Zhang, D. Hao, Z. Zhang, L. Wu, M. Li, S. Feng, X. Xu, F. Liu, X. Chen, Z. Bo, *Chem. Mater.*, 2018, **30**, 4307.
49. T. Dai, P. Lei, B. Zhang, J. Zhou, A. Tang, Y. Geng, Q. Zeng, E. Zhou, *ACS Appl. Mater. Interfaces*, 2021, **13**, 30756.

50. S. Li, L. Ye, W. Zhao, X. Liu, J. Zhu, H. Ade, J. Hou, *Adv. Mater*., 2017, **29**, 1704051.
51. W. Zhao, D. Qian, S. Zhang, S. Li, O. Inganäs, F. Gao, J. Hou, *Adv. Mater*., 2016, **28**, 4734.
52. Z. Zhang, J. Yu, X. Yin, Z. Hu, Y. Jiang, J. Sun, J. Zhou, F. Zhang, T. P. Russell, F. Liu, W. Tang, *Adv. Funct. Mater*., 2018, **28**, 1705095.
53. S. Li, L. Ye, W. Zhao, S. Zhang, S. Mukherjee, H. Ade, J. Hou, *Adv. Mater*., 2016, **28**, 9423.
54. H. Yao, L. Ye, J. Hou, B. Jang, G. Han, Y. Cui, G. M. Su, C. Wang, B. Gao, R. Yu, H. Zhang, Y. Yi, H. Y. Woo, H. Ade, J. Hou, *Adv. Mater*., 2017, **29**, 1700254.
55. W. Li, L. Ye, S. Li, H. Yao, H. Ade, J. Hou, *Adv. Mater*., 2018, **30**, 1707170.
56. X. Li, G. Huang, N. Zheng, Y. Li, X. Kang, S. Qiao, H. Jiang, W. Chen, R. Yang, *Sol. RRL*, 2019, **3**, 1900005.
57. T.-W. Chen, K.-L. Peng, Y.-W. Lin, Y.-J. Su, K.-J. Ma, L. Hong, C.-C. Chang, J. Hou, C.-S. Hsu, *J. Mater. Chem. A*, 2020, **8**, 1131.
58. K.-K. Liu, X. Xu, J.-L. Wang, C. Zhang, G.-Y. Ge, F.-D. Zhuang, H.-J. Zhang, C. Yang, Q. Peng, J. Pei, *J. Mater. Chem. A*, 2019, **7**, 24389.
59. Y. Gao, Z. Shen, F. Tan, G. Yue, R. Liu, Z. Wang, S. Qu, Z. Wang, W. Zhang, *Nano energy*, 2020, **76**, 104964.
60. H. Zhang, H. Yao, J. Hou, J. Zhu, J. Zhang, W. Li, R. Yu, B. Gao, S. Zhang, J. Hou, *Adv.Mater*., 2018, **30**, 1800613.